J. Biol. Macromol., **18**(2), 15-22 (2018)

Review

Microcrystal-carrier matrices for serial crystallography

Michihiro Sugahara[1,2*], Takanori Nakane[3,4], Eriko Nango[1,2], Kensuke Tono[5], Makina Yabashi[1] and So Iwata[1,2]

[1]RIKEN SPring-8 Center, 1-1-1 Kouto, Sayo-cho, Sayo-gun, Hyogo 679-5148, Japan
[2]Department of Cell Biology, Graduate School of Medicine, Kyoto University, Yoshidakonoe-cho, Sakyo-ku, Kyoto 606-8501, Japan
[3]Department of Biological Sciences, Graduate School of Science, The University of Tokyo, 7-3-1 Hongo, Bunkyo-ku, Tokyo 113-0033, Japan
[4](Present Address) MRC Laboratory of Molecular Biology, Cambridge Biomedical Campus, Francis Crick Avenue, Cambridge CB2 OQH, UK
[5]Japan Synchrotron Radiation Research Institute, 1-1-1 Kouto, Sayo-cho, Sayo-gun, Hyogo 679-5198, Japan,

Received May 18, 2018

Serial femtosecond crystallography (SFX) with femtosecond X-ray pulses from X-ray free-electron lasers (XFELs) offers a route to overcome radiation damage to small protein crystals via the 'diffraction-before-destruction' approach. A single-pulse X-ray exposure completely destroys individual crystals; therefore, fresh specimens must be supplied for subsequent X-ray pulses to continue data acquisition. A matrix method using protein crystal carriers, such as grease and oil-free hydrogel media, has been developed for serial sample loading. The micro-extrusion technique employing matrices allows the structure determination of a wide variety of proteins with low sample consumption, typically less than 1 mg. This offers new opportunities for time-resolved studies of light-driven structural changes and chemical dynamics using pump-probe techniques at XFEL and synchrotron facilities.

Key words: X-ray free-electron laser, serial femtosecond crystallography, protein crystal, viscous carrier media, grease matrix

Serial crystallography at XFEL and other facilities

High resolution structures provide key insights into functions and mechanisms of biomolecules, for example, substrate recognition, catalysis and regulation. This information can then be used to control their functions by drugs or exploit them as tools in biology and chemistry. High brilliance synchrotron-based X-ray sources, sensitive two-

*To whom correspondence should be addressed: msuga@spring8.or.jp

Fig. 1. The SPring-8 Angstrom Compact free electron LAser (SACLA), RIKEN SPring-8 Center, Hyogo, Japan.

dimensional detectors and cryo-cooling techniques have facilitated high resolution structure determination of proteins. Nevertheless, specimens analysed using traditional X-ray crystallography techniques suffer from radiation-induced structural changes. XFELs have created new opportunities in structural biology by allowing acquisition of diffraction patterns before the onset of X-ray radiation damage via ultra-fast X-ray exposures in the femtosecond (fs) region. This is known as 'diffraction before destruction'[(1)]. Several XFEL facilities have been constructed; the Linac Coherent Light Source (LCLS) in USA started user operation in 2009 as the first hard X-ray FEL. The SPring-8 Angstrom Compact free-electron LAser (SACLA) in Japan followed in 2012. PAL-XFEL in South Korea and the European XFEL in Germany started in 2017, and the SwissFEL in Switzerland is planned for 2019.

SACLA[(2)] **(Fig. 1)** provides ultrafast X-ray pulses with a duration shorter than 10 fs at a wide photon energy range from 4 to 20 keV (4–15 keV for user operation)[(3)]. The SACLA facility is designed to operate up to five beamlines (BLs) with independent undulators. As of 2018, three BLs can be operated simultaneously. User operation of BL3 for hard X-ray FEL and BL1 for wide-range spontaneous radiation began in 2012. The BL1 has been upgraded to produce soft X-ray FEL with a dedicated linac called SCSS+. The upgraded BL1 has been open to users since 2016. The BL2 was constructed in 2013 as the second hard X-ray FEL beamline. Parallel operation of BL2 and BL3 began in 2017.

Serial femtosecond crystallography (SFX) **(Fig. 2)** has been established at the LCLS[(4–7)]. A single XFEL pulse completely destroys small individual crystals, meaning that each specimen survives only for a single shot, necessitating the supply of fresh crystals for subsequent X-ray pulses to continue data acquisition. SFX allows data collection from small protein crystals on the micrometre to submicrometer scales to determine room-temperature structures[(8–15)]. SFX also enables time-resolved experiments

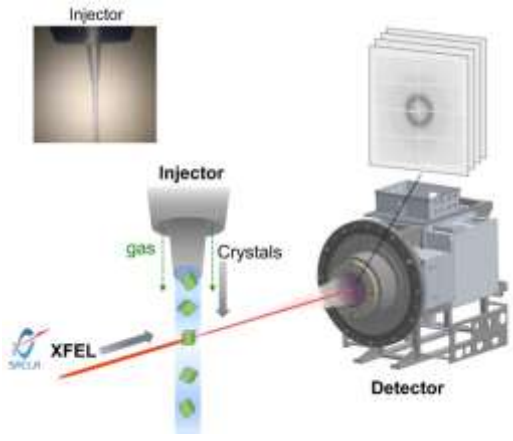

Fig. 2. Serial femtosecond crystallography at SACLA. Fresh nano/microcrystals are supplied for subsequent X-ray pulses.

even with femtosecond time resolution. Reactions are typically triggered by an optical laser or substrate mixing[16–22]. As a diffraction pattern is recorded with a single X-ray pulse, non-cyclic, irreversible processes can be studied. Data collection from smaller crystals, made possible by SFX, has the advantage of probing more spatially uniform, temporally synchronised reactions, as smaller crystal volume allows better laser permeation and faster substrate diffusion throughout the crystal. Serial crystallography is also being adapted to synchrotron radiation[23,24].

Serial sample loading for serial crystallography

A gas dynamic virtual nozzle (GDVN), which generates a liquid jet with a co-flowing gas to stabilise and reduce the jet diameter, is mainly used to inject small protein crystals in their mother liquor into the XFEL beam at LCLS[25]. A GDVN has also been applied to mix-and-inject serial crystallography to study enzyme–substrate interactions in real-time[26–29]. In the first stage of the SFX research at SACLA, a GDVN-based liquid jet injector was installed into an experimental platform DAPHNIS (Diverse Application Platform for Hard X-ray Diffraction in SACLA), which consists of a sample chamber, a fluid injector and a custom-built 4-megapixel detector with multi-port CCD sensors[30]. However, continuous flow extraction with a liquid jet injector requires a relatively high flow speed of ~10 m/sec. At lower rates, the flow is disrupted by the surface tension of water, resulting in dripping. Thus, a suitably fast liquid jet consumes 10–100 mg of protein sample, and this high rate of sample consumption impedes structure determination of proteins whose production is often difficult.

For membrane proteins, Uwe Weierstall and coworkers at Arizona State University developed a lipidic cubic phase (LCP) injector. The viscosity of LCP means that it can be operated at a lower flow rate of ~0.2 µl/min[31] , a significant improvement on GDVN injectors. Using the same basic concept, we developed an injector that extrudes viscous samples in LCP. The injector consists of a hydraulic cylinder, a removable sample reservoir and a nozzle, and is mounted in the DAPHNIS chamber. In order to inject protein crystals of a wide variety of soluble and membrane proteins at low flow rates, we have introduced mineral oil-based grease as a protein carrier (grease matrix) in SFX[14]. Micro-extrusion of small protein crystals using a variety of grease[14,32,33] achieves a stable sample stream at a low flow rate of ~0.5 µl/min or less, which reduces sample consumption to less than 1 mg.

Highly viscous crystal carrier media

Mineral oil-based grease[14] gives adequate protection against cracking and dissolution of protein crystals, which is the reason why mineral oil is used as a versatile cryoprotectant for protein crystals in X-ray crystallography[34]. We have also introduced Super Lube synthetic grease[32] and Super Lube nuclear grade approved grease (nuclear grease)[33], which give lower background scattering than the mineral

oil-based grease. Although grease media have potential as a versatile matrix carrier, even the nuclear grease produces strong X-ray scattering in the resolution range of 4–5 Å, hence increasing noise levels. To improve the signal-to-noise ratio of diffraction data, we have introduced a hydrogel matrix technique using hyaluronic acid[32] and hydroxyethyl cellulose[33]. We confirmed that the hydrogel matrices give lower background scattering compared to the scattering generated by a grease. In the matrix technique, the first step is to find a suitable carrier medium for the protein crystals. We occasionally observed cracking and dissolution of soluble and membrane protein crystals in the grease or hydrogel matrix, respectively. Grease and hydrogel crystal carriers are therefore complementary.

In the grease matrix method, grease and crystals are mixed together typically in a ratio of 9:1 (*v/v*) **(Fig. 3)**. For example, after a 100-µl sample of crystal suspension (e.g. a crystal density of ~10^7 crystals/ml) **(Fig. 3a)** is centrifuged, a 90-µl aliquot of supernatant solution is removed, in order to increase the crystal density. A 10-µl aliquot of the crystal solution is dispensed into 90 µl of grease on a glass slide and then mixed with a spatula **(Fig. 3b)**. Typically, ~30 µl of protein crystals (size 5–20 µm; crystal density ~10^7 crystals/ml) are dispersed in a matrix and mounted on an injector. The flow rate is usually ~0.5 µl/min through a 100-µm-i.d. injector nozzle **(Fig. 3c)**. Up to 100,000 images can be collected during 1 hour of data collection at 30 Hz. Assuming an index rate of 20% to 30%, 20,000–30,000 indexed patterns can be collected, which provides sufficient multiplicity for high resolution structure determination. Although higher hit rates can be achieved with increased crystal densities, this would cause multiple crystal hits in one XFEL shot, resulting in spot overlaps and mis-indexing. A crystal density up to ~10^7 crystals/ml is ideal for SFX data collection under our experimental conditions using 75–100-µm-i.d. nozzles.

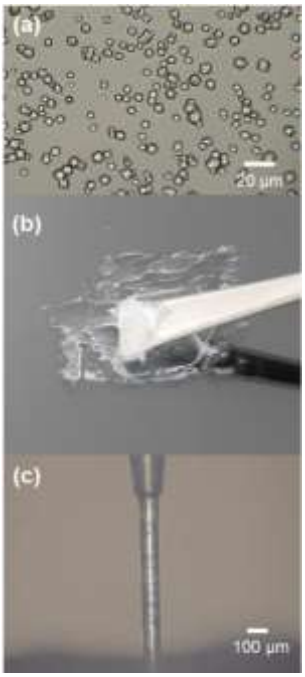

Fig. 3. Grease matrix method. (**a**) Proteinase K microcrystals used for SFX measurements. (**b**) Grease and crystals are dispensed on a glass slide and then mixed with a spatula. (**c**) Sample extrusion through a 100-µm-i.d. injector nozzle.

Example applications

To date, we have demonstrated the utility of grease matrices in SFX at SACLA using a wide variety of soluble and membrane proteins: lysozyme, glucose isomerase, thaumatin, fatty acid-binding protein type 3 and proteinase K[14,32,33,35], copper nitrite reductase[15], photosystem II (PSII)[20], luciferin-regenerating enzyme[36], the photoswitchable fluorescent protein IrisFP[37], bacteriorhodopsin[38], bacterial phytochrome[39], the stem domain of human POMGnT1 and galectin[40], and thermolysin[41]. The micro-extrusion technique with grease matrices is the most common injection method for SFX at SACLA.

Using the hydroxyethyl cellulose matrix and 13 keV (0.95 Å wavelength) XFEL pulses from SACLA[42], the proteinase K crystal structure was determined at 1.20-Å resolution **(Fig. 4)**[43], a resolution allowing us to visualise even hydrogen atoms[44].

Although most structures in SFX have been phased by molecular replacement using homologous structures, *de novo* phasing from heavy atom-derivatised crystals has also been demonstrated in many studies[15,33,36,38,40,45–49]. Using grease matrix, *de novo* phasing was accomplished by Hg-SIRAS (single isomorphous replacement with anomalous scattering)[36], Cu-SAD (single-wavelength anomalous diffraction)[15], I-SAD[38], Se-/Hg-SAD[40] and Gd-MAD (multi-wavelength anomalous diffraction)[49] at SACLA. Additionally, we demonstrated *de novo* structure determination of proteinase K from Pr-derivatised crystals using hydroxyethyl cellulose matrix[33]. A total of 2,000 indexed patterns (native/derivative: 1,000/1,000) were sufficient for Pr-SIR and SIRAS phasing of proteinase K. Native sulfur SAD phasing was also successful with SFX[35,46,50]. Using grease matrix, we demonstrated that the structure of lysozyme can be determined by SAD phasing from the anomalous signal of sulfur in the protein and chlorine in the buffer[35]. For native SAD phasing, we collected 150,000 indexed patterns to 2.2 Å resolution at 7 keV photon energy (1.77 Å wavelength). These results established that our matrix technique is compatible with accurate measurements of weak anomalous signals.

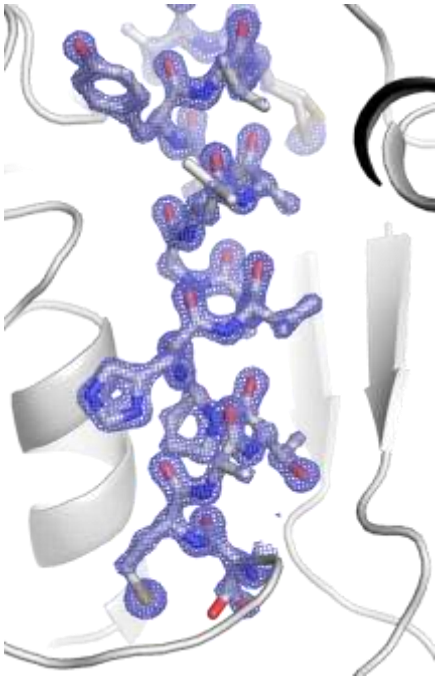

Fig. 4. A close-up view of proteinase K at 1.20 Å-resolution with a 2Fo–Fc electron-density map contoured at the 2.7σ level.

Applications to time-resolved studies

The femtosecond X-ray pulses are instrumental in observing time-dependent phenomena using a pump-probe technique. The temporal resolution of pump-probe experiments is determined by the duration of the pump as well as the probe. In a typical scheme of optical pump–X-ray probe experiments, the probe X-ray pulse follows the pump pulse after a desired time delay. The time-resolved experiment requires that pumped crystals remain in the X-ray interaction region and that the probed crystals flow out of the region before the next X-ray probe pulse. Thus, optical pump–X-ray probe experiments require a stable stream with a constant flow rate. In the first time-resolved SFX study at SACLA, Nango et al. reported the conformational changes of bacteriorhodopsin (crystallised in LCP) at 13 time points from nanoseconds to milliseconds following photoactivation[19], using nanosecond pump-probe device for time-resolved SFX[51]. Since our matrix method achieves a stable sample flow with low sample consumption, it is suited for time-resolved studies using pump-probe techniques. The structural changes of photosystem II (PSII) induced by 2-flash illumination have been captured at a resolution of 2.35 Å with the grease matrix technique[20]. The structure of cytochrome P450 nitric oxide reductase during catalytic reactions has been determined using a combination of a photosensitive caged-compound (caged-NO) and the hydroxyethyl cellulose matrix[21].

A wide variety of the crystal carriers for serial sample loading have been reported in recent years; Vaseline (petroleum jelly)[52], agarose[53], sodium carboxymethyl cellulose, the thermo-reversible block polymer Pluronic F-127[54] and a high-molecular-weight poly(ethylene oxide) (PEO)[55]. One type of carrier media is not always compatible with a given crystal, causing cracking and dissolution of crystals due to physical or chemical stress, such as osmotic shock. A wide repertoire of carrier media will, therefore, be a valuable resource for a wide variety of proteins.

Nowadays, synchrotron-based serial crystallography is also performed using a variety of viscous carrier media[23,24,52,54,55]. Thus, the technique of sample loading using viscous media has become increasingly important not only in SFX but also in serial millisecond crystallography using synchrotron radiation. Furthermore, our matrix-based approach should be applicable to non-protein targets such as organic and inorganic nano/micro crystals.

Acknowledgements

This work was supported by the X-ray Free-Electron Laser Priority Strategy Program (MEXT) and partly by Platform Project for Supporting Drug Discovery and Life Science Research from AMED (grant JP17am0101070). The authors thank all the members of the SACLA-SFX project.

References

1. Neutze, R., Wouts, R., van der Spoel, D., Weckert, E. & Hajdu, J. Potential for biomolecular imaging with femtosecond X-ray pulses. *Nature* **406**, 752–757 (2000).
2. Ishikawa, T. *et al.* A compact X-ray free-electron

laser emitting in the sub-ångström region. *Nat. Photonics* **6**, 540–544 (2012).
3. Yabashi, M., Tanaka, H. and Ishikawa, T. Overview of the SACLA facility. *J. Synchrotron Rad*. **22**, 477–484 (2015).
4. Chapman, H. N. *et al*. Femtosecond X-ray protein nanocrystallography. *Nature* **470**, 73–77 (2011).
5. Emma, P. *et al*. First lasing and operation of an ångstrom-wavelength free-electron laser. *Nat. Photonics* **4**, 641–647 (2010).
6. Barty, A. *et al*. Self-terminating diffraction gates femtosecond X-ray nanocrystallography measurements. *Nat. Photonics* **6**, 35–40 (2012).
7. Schlichting, I. Serial femtosecond crystallography: the first five years. *IUCrJ* **2**, 246–255 (2015).
8. Johansson, L. C. *et al*. Lipidic phase membrane protein serial femtosecond crystallography. *Nat. Methods* **9**, 263–265 (2012).
9. Redecke, L. *et al*. Natively inhibited *Trypanosoma brucei* cathepsin B structure determined by using an X-ray laser. *Science* **339**, 227–230 (2013).
10. Liu, W. *et al*. Serial femtosecond crystallography of G protein–coupled receptors. *Science* **342**, 1521–1524 (2013).
11. Kang, Y. *et al*. Crystal structure of rhodopsin bound to arrestin by femtosecond X-ray laser. *Nature* **523**, 561–567 (2015).
12. Zhang, H. *et al*. Structure of the Angiotensin receptor revealed by serial femtosecond crystallography. *Cell* **161**, 833–844 (2015).
13. Zhou, Q. *et al*. Architecture of the synaptotagmin–SNARE machinery for neuronal exocytosis. *Nature* **525**, 62–67 (2015).
14. Sugahara, M. *et al*., Grease matrix as a versatile carrier of proteins for serial crystallography. *Nat. Methods* **12**, 61–63 (2015).
15. Fukuda, Y. *et al*. Redox-coupled proton transfer mechanism in nitrite reductase revealed by femtosecond crystallography. *Proc. Natl. Acad. Sci. USA*. **113**, 2928–2933 (2016).
16. Tenboer, J. *et al*. Time-resolved serial crystallography captures high-resolution intermediates of photoactive yellow protein. *Science* **346**, 1242–1246 (2014).
17. Kupitz, C. *et al*. Serial time-resolved crystallography of photosystem II using a femtosecond X-ray laser. *Nature* **513**, 261–265 (2014).
18. Barends, T. R. M. *et al*. Direct observation of ultrafast collective motions in CO myoglobin upon ligand dissociation. *Science* **350**, 445–450 (2015).
19. Nango, E. *et al*. A three dimensional movie of structural changes in bacteriorhodopsin. *Science* **354**, 1552–1557 (2016).
20. Suga, M. *et al*. Light-induced structural changes and the site of O=O bond formation in PSII caught by XFEL. *Nature* **543**, 131–135 (2017).
21. Tosha, T. *et al*. Capturing an initial intermediate during the P450nor enzymatic reaction using time-resolved XFEL crystallography and caged-substrate. *Nat. Commun.* **8**, 1585 (2017).
22. Coquelle, N. *et al*. Chromophore twisting in the excited state of a photoswitchable fluorescent protein captured by time-resolved serial femtosecond crystallography. *Nat. Chemistry* **10**, 31–37 (2018).
23. Stellato, F. *et al*. Room-temperature macromolecular serial crystallography using synchrotron radiation. *IUCrJ* **1**, 204–212 (2014).
24. Nogly, P. *et al*. Lipidic cubic phase serial millisecond crystallography using synchrotron radiation. *IUCrJ* **2**, 168–176 (2015).
25. DePonte, D. P. *et al*. Gas dynamic virtual nozzle for generation of microscopic droplet streams. *J. Phys. D Appl. Phys*. **41**, 195505 (2008).
26. Wang, D., Weierstall, U., Pollackb, L. & Spencea, J. Double-focusing mixing jet for XFEL study of chemical kinetics. *J. Synchrotron Rad*. **21**, 1364–1366 (2014).
27. Calvey, G.D., Katz, A.M., Schaffer, C.B. & Pollack, L. Mixing injector enables time-resolved crystallography with high hit rate at X-ray free electron lasers. *Struct. Dyn*. **3**, 054301 (2016).
28. Stagno, J. R. *et al*. Structures of riboswitch RNA reaction states by mix-and-inject XFEL serial crystallography. *Nature* **541**, 242–246 (2017).
29. Kupitz, C. *et al*. Structural enzymology using X-ray free electron lasers. *Struct. Dyn*. **4**, 044003 (2017).
30. Tono, K. *et al*. Diverse application platform for hard X-ray diffraction in SACLA (DAPHNIS): application to serial protein crystallography using an X-ray free-electron laser. *J. Synchrotron Rad*. **22**, 532–537 (2015).
31. Weierstall, U. *et al*. Lipidic cubic phase injector facilitates membrane protein serial femtosecond crystallography. *Nat. Commun*. **5**, 3309 (2014).
32. Sugahara, M. *et al*. Oil-free hyaluronic acid matrix for serial femtosecond crystallography. *Sci. Rep*. **6**, 24484 (2016).
33. Sugahara, M. *et al*. Hydroxyethyl cellulose matrix applied to serial crystallography. *Sci. Rep*. **7**, 703 (2017).
34. Hope, H. Cryocrystallography of biological macromolecules: a generally applicable method. *Acta Crystallogr. B*. **44**, 22–26 (1988).
35. Nakane, T. *et al*. Native sulfur/chlorine SAD phasing for serial femtosecond crystallography. *Acta Crystallogr. D.* **71**, 2519– 2525 (2015).
36. Yamashita, K. *et al*. An isomorphous replacement

method for efficient de novo phasing for serial femtosecond crystallography. *Sci. Rep*. **5**, 14017 (2015).
37. Colletier, J. P. *et al*. Serial femtosecond crystallography and ultrafast absorption spectroscopy of the photoswitchable fluorescent protein IrisFP. *J. Phys. Chem. Lett*. **7**, 882−887 (2016).
38. Nakane, T. *et al*. Membrane protein structure determination by SAD, SIR or SIRAS phasing in serial femtosecond crystallography using a novel iododetergent. *Proc. Natl. Acad. Sci. USA*. **113**, 13039–13044 (2016).
39. Edlund, P. *et al*. The room temperature crystal structure of a bacterial phytochrome determined by serial femtosecond crystallography. *Sci. Rep*. **6**, 35279 (2016).
40. Yamashita, K. *et al*. Experimental phase determination with selenomethionine or mercury-derivatization in serial femtosecond crystallography. *IUCrJ* **4**, 639–647 (2017).
41. Naitow, H. *et al*. Protein–ligand complex structure from serial femtosecond crystallography using soaked thermolysin microcrystals and comparison with structures from synchrotron radiation. *Acta Crystallogr. D.* **73**, 702–709 (2017).
42. Tono, K. *et al*. Beamline, experimental stations and photon beam diagnostics for the hard x-ray free electron laser of SACLA. *New J. Phys*. **15**, 083035 (2013).
43. Nakane, T. *et al*. Data processing pipeline for serial femtosecond crystallography at SACLA. *J. Appl. Crystallogr*. **49**, 1035–1041 (2016).
44. Masuda, T. *et al*. Atomic resolution structure of serine protease proteinase K at ambient temperature. *Sci. Rep*. **7**, 45604 (2017).
45. Barends, T. R. M. *et al*. *De novo* protein crystal structure determination from X-ray free-electron laser data. *Nature* **505**, 244–247 (2014).
46. Nass, K. *et al*. Protein structure determination by single-wavelength anomalous diffraction phasing of X-ray free-electron laser data. *IUCrJ* **3**, 180–191 (2016).
47. Colletier, J. P. *et al*. *De novo* phasing with X-ray laser reveals mosquito larvicide BinAB structure. *Nature* **539**, 43–47 (2016).
48. Hunter, M. S. *et al*. Selenium single-wavelength anomalous diffraction *de novo* phasing using an X-ray-free electron laser. *Nat. Commun*. **7**, 13388 (2016).
49. Gorel, A. *et al*. Multi-wavelength anomalous diffraction *de novo* phasing using a two-colour X-ray free-electron laser with wide tunability. *Nat. Commun*. **8**, 1170 (2017).
50. Batyuk, A. *et al*. Native phasing of x-ray free-electron laser data for a G protein–coupled receptor. *Sci. Adv*. **2**, e1600292 (2016).
51. Kubo, M. *et al*. Nanosecond pump–probe device for time-resolved serial femtosecond crystallography developed at SACLA. *J. Synchrotron Rad. 24*, 1086–1091 (2017).
52. Botha, S. *et al*. Room-temperature serial crystallography at synchrotron X-ray sources using slowly flowing free-standing high-viscosity microstreams. *Acta Crystallogr. D*. **71**, 387–397 (2015).
53. Conrad, C. E. *et al*. A novel inert crystal delivery medium for serial femtosecond crystallography. *IUCrJ* **2**, 421–430 (2015).
54. Kovácsová, G. *et al*. Viscous hydrophilic injection matrices for serial crystallography. *IUCrJ* **4**, 400–410 (2017).
55. Martin-Garcia, J. M. *et al*. Serial millisecond crystallography of membrane and soluble protein microcrystals using synchrotron radiation. *IUCrJ* **4**, 439–454 (2017).

Communicated by Komori Hirofumi